Tumor Biol. (2016) 37:2473–2480
DOI 10.1007/s13277-015-4072-0

ORIGINAL ARTICLE

LIM domain only 2 induces glioma invasion via cytosolic p27^{KIP1}

Cheol Gyu Park[1] · **Young-Woo Sohn**[1] · **Eun-Jung Kim**[1,2] · **Sung-Hak Kim**[1,3] · **Sung-Chan Kim**[4] · **Hyunggee Kim**[1,2]

Received: 18 June 2015 / Accepted: 13 September 2015 / Published online: 18 September 2015

Abstract High-grade gliomas are considered the most malignant of brain tumors and have a poor prognosis. In a previous study, we showed that LIM domain only 2 (LMO2) regulates glioma stem cell properties and tumor angiogenesis and gave rise to highly invasive glioma xenografts. Glioma invasion in the surrounding parenchymal tissues is a major hurdle with respect to eliminating glioma by surgery. Invasive glioma cells are considered one of the main culprits for the recurrence of tumors after therapies. In the current study, we focused on determining the molecular mechanism(s) by which LMO2 regulates glioma cell migration and invasion. Forced expression of LMO2 in human U87MG glioma cells led to glioma invasion, as determined by in vivo xenograft assays and enhanced in vitro migration and invasion. LMO2 was associated with increased levels of cytosolic p27^{Kip1} protein. LMO2 possibly induced the stabilization and augmented interactions between p27^{Kip1} and RhoA. We knocked down the expression of p27^{Kip1}, which led to a decrease in LMO2-driven glioma cell migration and invasion. Taken together, our findings indicate that LMO2 promotes glioma cell migration and invasion by increasing the levels of cytosolic p27^{Kip1}.

Keywords Cell invasion · Cell migration · Glioma · LMO2 · p27^{Kip1} · RhoA

✉ Sung-Chan Kim
biokim@hallym.ac.kr

✉ Hyunggee Kim
hg-kim@korea.ac.kr

[1] Department of Biotechnology, School of Life Science and Biotechnology, Korea University, Seoul 136-713, Republic of Korea

[2] Institute of Animal Molecular Biotechnology, Korea University, Seoul 136-713, Republic of Korea

[3] Department of Neurological Surgery, James Comprehensive Cancer Center, The Ohio State University, Columbus, OH 43210, USA

[4] Department of Biochemistry, College of Medicine, Hallym University, Chuncheon 200-702, Republic of Korea

Introduction

High-grade glioma (HGG) is one of the most devastating brain tumors, with a median survival period of 12–14 months [1]. Histologically, HGG tumors are highly invasive and are characterized by intrusions into surrounding brain tissues [2]. HGG cells often migrate to the distal region of the brain via white matter tracts and blood vessels [3, 4]. Because of these invasive and migratory capabilities, conventional therapies such as surgical resection, chemotherapy, and radiotherapy often fail to eliminate disseminated HGG cells. These remaining infiltrative tumor cells result in the recurrence of brain tumors and are responsible for the poor prognosis associated with HGG [5].

Cell migration is a multistep process involving leading edge protrusion, lamellipodium, and tail retraction. These processes are regulated by diverse intracellular signaling molecules [6]. The Rho-type GTPases play an important role in modulating cell motility and shape. Among them, Rho, Rac, and Cdc42 are key components in controlling actin cytoskeleton dynamics [7]. Rho regulates the contraction of actin-myosin filaments, while Cdc42 and Rac regulate actin polarity. The dysregulation of these proteins has been reported in many human malignancies, including skin [8], bladder [9], and brain cancer [10, 11].

The LIM domain only 2 (LMO2) protein is a member of the LMO family. It does not bind to DNA but acts as a bridging molecule in a multi-protein complex containing LDB1,

SCL/TAL1, E2a, and GATA1. This complex binds DNA through the zinc fingers of GATA1 and the basic helix-loop-helix components of TAL1 and E47 [12–14]. LMO2 functions as an effector for gene expression and is usually required for enhanced transcription [15]. Results from a number of studies have revealed that LMO2 plays an essential role in hematopoiesis and angiogenesis during early embryonic development [16–18].

$p27^{Kip1}$ is known to have dual functions in the regulation of cell cycle and cell migration, based on its subcellular localization. In the nucleus, $p27^{Kip1}$ binds to cyclin E/CDK2 and inhibits G1-S transition [19]. In early G1, nuclear $p27^{Kip1}$ is phosphorylated at serine 10 by mitogenic signals, which facilitates its nuclear export [20, 21]. Oncogenic signals such as PI3K/AKT and RAS/MAPK phosphorylate cytosolic $p27^{Kip1}$ at threonines 157 and 198, leading to $p27^{Kip1}$ stabilization. Cytosolic $p27^{Kip1}$ promotes cell proliferation via interaction with cyclin D/CDK4 [22] and cell migration via inhibition of RhoA/ROCK signaling [23].

In a previous study, we showed that LMO2 promotes the initiation and progression of tumors by inducing glioma stem cell properties and tumor angiogenesis [24]. Ectopic expression of LMO2 in astrocytes from Ink4a/Arf knockout mice gave rise to highly invasive gliomas [24]. We investigated whether LMO2-driven glioma cell migration and invasion is a common event among human glioma cells. We found that LMO2 induces glioma cell migration and invasion by stabilizing the cytosolic $p27^{Kip1}$ protein.

Material and methods

Cell culture

The human glioma cell line U87MG was purchased from the American Type Culture Collection (Manassas, VA, USA). Cell cultures were maintained in high-glucose Dulbecco's modified Eagle's medium (Lonza, Switzerland) supplemented with 10 % fetal bovine serum (FBS) (Serana, Australia) and incubated at 37 °C/5 % CO_2.

Plasmids, transfection, and retroviral infection

The gene sequence encoding the LMO2 protein was cloned into the pLL-CMV-puro lentivirus vector. These recombinant vectors were transfected into the human embryonic kidney cell line 293FT (Invitrogen, Carlsbad, CA, USA) with PolyExpress™ Transfection Reagent (Excellgen, Rockville, MD, USA) according to the manufacturer's instructions. Lentiviruses were concentrated with Lenti-X™ Concentrator (Clontech, Japan). Cells were also transfected with $p27^{KIP1}$-specific short-hairpin RNAs (shRNAs; 5′-AAT GGA CAT CCT GTA TAA GCA-3′), which were cloned into pSUPER-GFP-Neo according to the manufacturer's instructions (Oligoengine, Seattle, WA, USA) [25].

Western blotting

Whole cell extracts, for western blotting, were prepared using RIPA lysis buffer (150 mM NaCl, 1 % Nonidet P-40, 0.1 % sodium dodecyl sulfate [SDS], and 50 mM Tris pH 7.4) supplemented with 1 mM β-glycerophosphate, 2.5 mM sodium pyrophosphate, 1 mM NaF, 1 mM Na_3VO_4, and a protease inhibitor cocktail (Roche, Switzerland). Total protein content was quantified using Bradford assay reagent (Bio-Rad, Hercules, CA, USA) according to the manufacturer's instructions. Equal quantities of total protein from each sample were separated by 12 % SDS-polyacrylamide gel electrophoresis (SDS-PAGE). Proteins were then transferred to polyvinylidene difluoride membranes (Millipore, Billerica, MA, USA). The membranes were blocked in 5 % (*w*/*v*) nonfat milk for 1 h at room temperature and then incubated with goat anti-LMO2 (diluted 1:1000; R&D Systems, Minneapolis, MN, USA), rabbit anti-p27 (1:2000; Santa Cruz Biotechnology, Dallas, TX, USA), rabbit anti-p-p27 (1:1000; R&D Systems), rabbit anti-p-Akt (1:1000; Signalway Antibody, Pearland, TX, USA), or mouse anti-human α-tubulin (1:10,000; Sigma-Aldrich, Missoula, MO, USA). Membranes were incubated with the appropriate horseradish peroxidase-conjugated secondary antibodies and signals visualized with a picoEPD Kit (Elpis Corporation Ltd., Seoul, South Korea). The results were quantified using ImageJ software (National Institute of Health, Bethesda, MD, USA).

Immunoprecipitation

U87MG cells were washed twice with cold phosphate-buffered saline (PBS) and lysed with 4 °C IP buffer (50 mM Tris pH 7.5, 1 % Nonidet P-40, 150 mM NaCl, 1 mM Na_3VO_4, and 2 mM EGTA) supplemented with a protease inhibitor cocktail (Roche). Cells were allowed to lyse on ice for 20 min and were then centrifuged (14,000 rpm, 20 min, 4 °C). Immunoprecipitation was conducted using an antibody against p27. Immune complexes were captured with A/G Plus-agarose Beads (Millipore). After two washes with IP buffer and one wash with PBS, bead-bound proteins were separated by 12 % SDS-PAGE. Subcellular fractions were prepared as described previously [26]. Briefly, whole cell extracts were prepared with Buffer A (10 mM HEPES pH 7.9, 10 mM KCl, 0.1 mM EDTA, 1 mM dithiothreitol [DTT], and 0.5 mM phenylmethylsulfonyl fluoride [PMSF]). After centrifugation (13,000 rpm, 10 min, 4 °C), supernatants were used as cytosolic extracts. These extracts were treated with Buffer B (20 mM HEPES pH 7.9, 0.4 M NaCl, 1 mM EDTA, 1 mM DTT, 1 mM PMSF, and 10 % NP-40) and centrifuged

(13,000 rpm, 10 min, 4 °C). The resulting supernatants were used as nuclear extracts.

Wound-healing assays

Cells were seeded into 6-well plates and grown until confluent. A linear wound was made by scraping a pipette tip across the cell monolayer, and the culture medium was replenished. At 18 h after the wound was made, images from four random fields of view were obtained using an Olympus microscope equipped with a camera (Olympus, Japan). Cell migration was calculated by measuring the gaps between cells.

Transwell invasion assays

The upper chambers of 24-well transwell plates (Corning Costar, Corning, NY, USA) were coated with Matrigel (BD Biosciences, Franklin Lakes, NJ, USA) and incubated at 37 °C for 24 h. The opposite side of upper chambers were coated with 0.2 % gelatin and incubated at 37 °C for at least 4 h. We then added 5×10^4 cells suspended in 100 μL of DMEM to each upper chamber. The lower chambers contained DMEM supplemented with 10 % FBS. Plates were incubated at 37 °C/5 % CO_2 for 3 days to allow cells to migrate through the Matrigel-coated filter membrane. Media in the upper chambers were removed carefully, and the filter was then stained with trypan blue. Cells that had migrated to the lower surface of the membrane were counted with the aid of a microscope.

Immunofluorescence assays

We fixed U87MG cells with 4 % paraformaldehyde for 10 min. Fixed cells were washed with PBS, permeabilized with 3 % Triton X-100 for 3 min, and blocked with 1 % BSA for 30 min. Samples were incubated with an antibody against p27 (diluted 1:200 in PBS) for overnight at 4 °C. The samples were then incubated with rabbit anti-mouse Alexa Fluor® 488 or Alexa Fluor 488® phalloidin (Invitrogen) at room temperature for 30 min and mounted with 4′,6-diamidino-2-phenylindole (diluted 1:1000 in PBS) for 5 min.

Orthotopic implantation assay

We harvested U87MG cells by trypsinization, washed them in PBS, and determined cell viability by trypan blue exclusion. We only used single-cell suspensions with >90 % viability for in vivo studies. Cells (5×10^4 in 3 μL of PBS) were stereotactically injected into the left striatum of 6-week-old BALB/c nu/nu nude mice (coordinates relative to the bregma: anterior–posterior +2 mm, medial–lateral +2 mm, and dorsal–ventral −3 mm). Mice whose body weight had decreased by >25 % were considered to have an intracranial tumor. Mice harboring tumors were perfused with PBS and 4 % paraformaldehyde. Intracranial tumor tissues were embedded in paraffin and sectioned (4-μm thickness) and stained with hematoxylin and eosin. All animal experiments were approved by the animal care committee of the College of Life Sciences and Biotechnology, Korea University (Seoul, Republic of Korea), and were performed in accordance with government and institutional guidelines and regulations.

Statistical analysis

Statistical analyses were performed with two-tailed Student's *t* test. A *P* value less than 0.05 or 0.01 was considered significant or very significant, respectively.

Results

LMO2 stimulates human U87MG glioma cell invasion in in vivo xenografts

We established human U87MG glioma cells that overexpressed LMO2 (U87MG-LMO2) and generated mouse xenografts by orthotopic implantation using U87MG and U87MG-LMO2 cells. The U87MG-LMO2 cells gave rise to highly invasive gliomas (Fig. 1a, b) compared with those from control U87MG cells (Fig. 1c, d). Tumors derived from U87MG-LMO2 cells had more finger-like protrusions in tumor margin than those from control U87MG cells (Fig. 1e). These results indicate that LMO2-mediated glioma invasion is a general feature of murine and human glioma cells.

LMO2 enhances in vitro migration and invasion of human U87MG glioma cells

Results from many studies have demonstrated that glioma cell invasion of xenografts is influenced by the tumor microenvironment [27]. We sought to determine whether LMO2 regulates glioma invasion by altering the glioma microenvironment or glioma cell per se. We examined the in vitro migratory ability of U87MG and U87MG-LMO2 cells using wound-healing assays. We found that U87MG-LMO2 cells migrated 2.2-fold faster than U87MG cells, as measured by cell migratory distances at 18 h after wounding (Fig. 2a). We then investigated the invasiveness of U87MG and U87MG-LMO2 cells and found that U87MG-LMO2 cells were more invasive than their U87MG counterparts (Fig. 2b). Taken together, these results indicate that LMO2 directly affects the migratory capabilities and invasiveness of glioma cells in vitro, and this is likely reflected in in vivo xenografts.

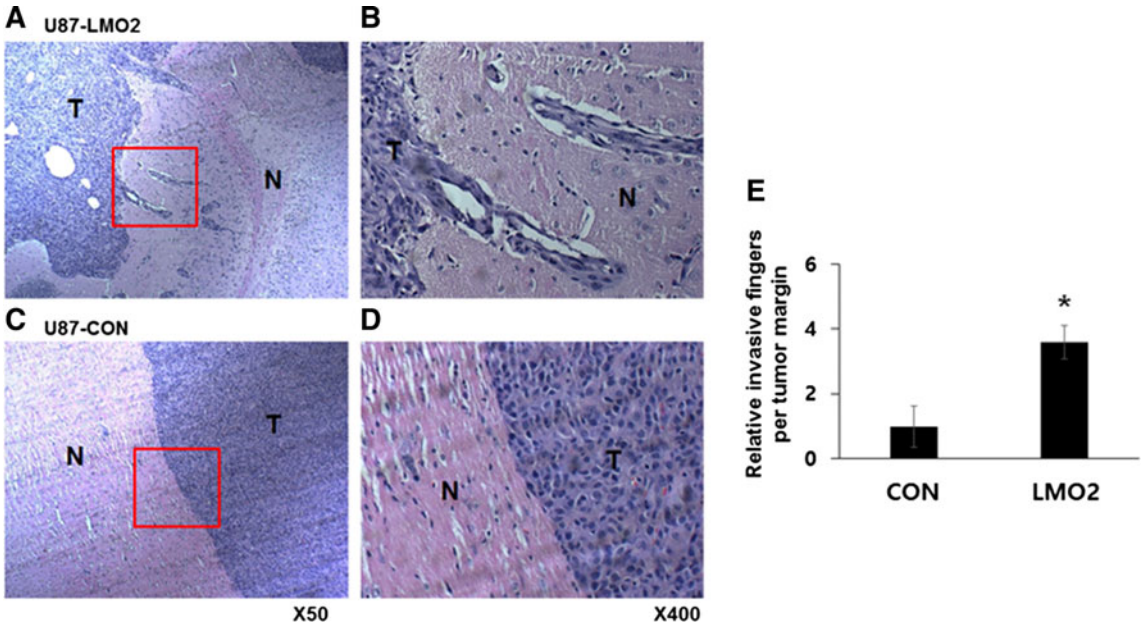

Fig. 1 LMO2 promotes U87MG invasion in in vivo xenografts. **a** A section stained with hematoxylin and eosin (H&E), showing a margin region of a mouse brain tumor xenograft derived from human U87MG-LMO2 cells (U87-LMO2; ×50 magnification). **b** The *red square* shown in **a** at ×400 magnification. **c** A section stained with H&E showing a margin region of a mouse brain tumor xenograft derived from U87MG cells (U87-CON; ×50 magnification). **d** The *red square* shown in **c** at ×400 magnification. *N* indicates normal brain regions in a mouse, while *T* indicates U87MG-derived brain tumor xenografts. **e** The number of invasive finger-like protrusions was counted randomly in the six fields of margin region of CON and LMO2 tumors. **P*<0.05 (*n*=6)

LMO2 increases cytosolic p27^{Kip1} levels and its interaction with RhoA

We previously demonstrated that accumulation of p27^{Kip1} in U87MG glioma cells induces glioma cell migration and invasion [25]. The p27^{Kip1} protein is a cyclin-dependent kinase (CDK) inhibitor in the nucleus and a cell migration inducer in the cytosol [23]. AKT-mediated phosphorylation of p27^{Kip1} at threonine 157 contributes to cytosolic localization and stabilization of p27^{Kip1} [28, 29]. Thus, we investigated whether p27^{Kip1} is involved in LMO2-driven glioma cell migration and invasion. Ectopic LMO2 expression in U87MG cells resulted in an increase in p27^{Kip1} and phosphorylated AKT levels (Fig. 3a). We also noticed an increase in the levels of

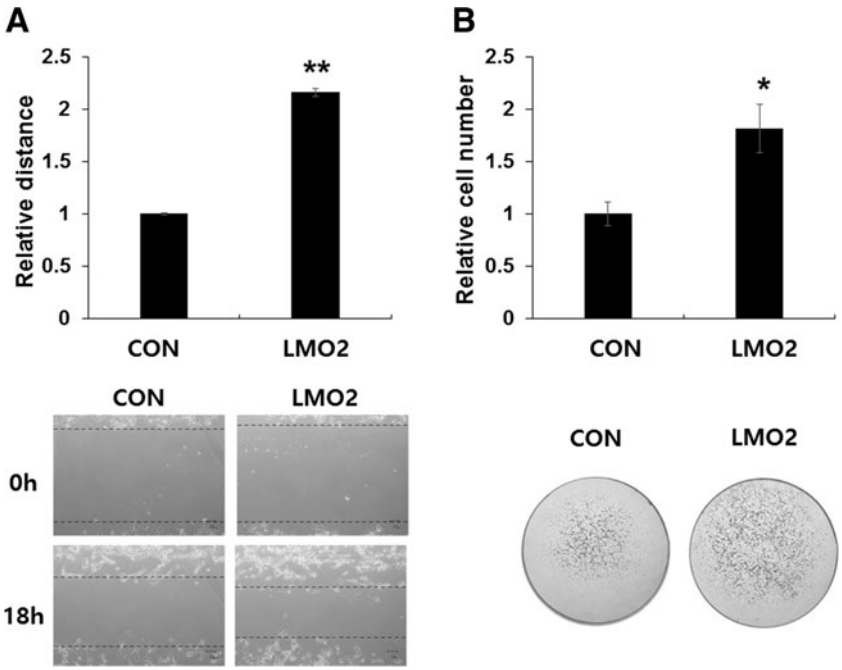

Fig. 2 LMO2 induces in vitro migration and invasion of U87MG glioma cells. **a** The in vitro migratory ability of U87MG (CON) and U87MG-LMO2 (LMO2) cells was examined using wound-healing assays. ***P*<0.01 (*n*=3). Representative images of wound healing assay are shown below. **b** The invasiveness of CON and LMO2 cells was determined in vitro using transwell invasion assays. **P*<0.05 (*n*=3). Representative images of transwell invasion assay are shown below

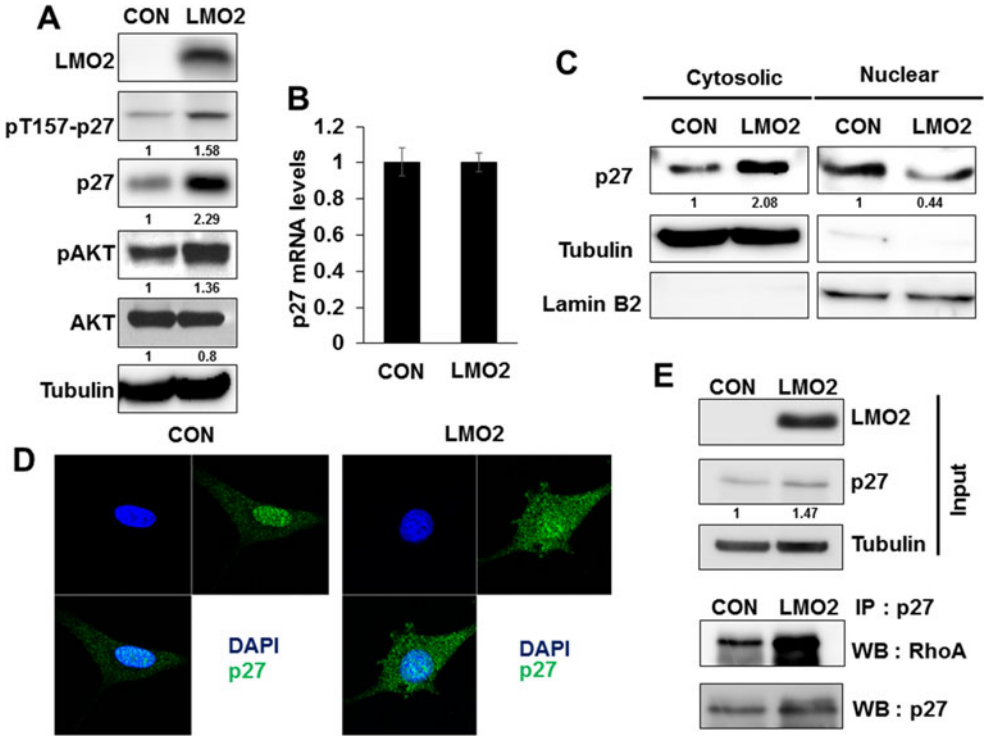

Fig. 3 LMO2 increases cytosolic $p27^{Kip1}$ and its interaction with RhoA. **a** Levels of total (p27) and $p27^{Kip1}$ phosphorylated at threonine157 (pT157-p27) in U87MG (CON), and U87MG-LMO2 (LMO2) cells were examined by western blotting. Protein expression levels were quantified using ImageJ software. **b** The levels of $p27^{Kip1}$ mRNAs in CON and LMO2 cells were analyzed by quantitative polymerase chain reaction assays. **c** The subcellular localization of $p27^{Kip1}$ in CON and LMO2 cells was examined by western blotting, with cytosolic and nuclear fractions of cell extracts. Tubulin and lamin B2 were used as cytosolic and nuclear protein markers, respectively. Protein expression levels were quantified using ImageJ software. **d** The subcellular localization of $p27^{Kip1}$ in CON and LMO2 cells as examined by immunofluorescence assays. **e** Levels of $p27^{Kip1}$, LMO2, and tubulin (indicated as *Input*) in CON and LMO2 cells were examined by western blotting. Following immunoprecipitation of CON and LMO2 cell extracts using an antibody against $p27^{Kip1}$, western blotting was conducted to assess the interaction between $p27^{Kip1}$ and RhoA proteins employing an antibody against RhoA. Expression levels of $p27^{Kip1}$ were quantified using ImageJ software

$p27^{Kip1}$ that were phosphorylated at threonine 157, which is involved in the stabilization of $p27^{Kip1}$ (Fig. 3a). We failed to observe any significant differences in $p27^{Kip1}$ mRNA levels between U87MG and U87MG-LMO2 cells (Fig. 3b). These results suggest that LMO2 might regulate $p27^{Kip1}$ protein levels through posttranslational modifications, but not by transcriptional regulation.

Cytosolic $p27^{Kip1}$ is associated with cell migration and invasion [25]; therefore, we examined the subcellular localization of $p27^{Kip1}$. Western blotting revealed that nuclear $p27^{Kip1}$ levels were decreased in U87MG-LMO2 cells compared with those in U87MG, but this difference was not significant (Fig. 3c). In contrast, cytosolic $p27^{Kip1}$ levels were increased to a greater extent in U87MG-LMO2 cells than in U87MG cells (Fig. 3c). Immunofluorescence assay results revealed that U87MG cells express $p27^{Kip1}$ mainly in the nucleus, while U87MG-LMO2 cells contain cytosolic and nuclear $p27^{Kip1}$ (Fig. 3d).

The $p27^{Kip1}$ protein is known to induce the migration of cells by directly interacting with RhoA, a key player in cellular migration via cytoskeleton remodeling [23]. We investigated whether interactions between $p27^{Kip1}$ and RhoA were increased in cells in which LMO2 was overexpressed. We observed that the interaction between these proteins was increased to a greater extent in U87MG-LMO2 cells compared with that in U87MG cells (Fig. 3e). Our results suggest that LMO2 might induce the migration and invasion of glioma cells via increases in cytosolic $p27^{Kip1}$ levels and through its interaction with RhoA.

LMO2 regulates glioma cell migration and invasion via cytosolic $p27^{Kip1}$

We examined whether an increase in $p27^{Kip1}$ levels was directly involved with LMO2-driven glioma cell migration and invasion. We confirmed that shRNA-mediated $p27^{Kip1}$ knockdown reduced the levels of total and phosphorylated $p27^{Kip1}$ in U87MG-LMO2 cells to levels seen in U87MG cells (Fig. 4a). Immunofluorescence using phalloidin, a hallmark of the lamellipodium F-actin network [30], revealed that the F-actin network in U87MG-LMO2 cells was obviously decreased following $p27^{Kip1}$ knockdown (Fig. 4b). Wound-

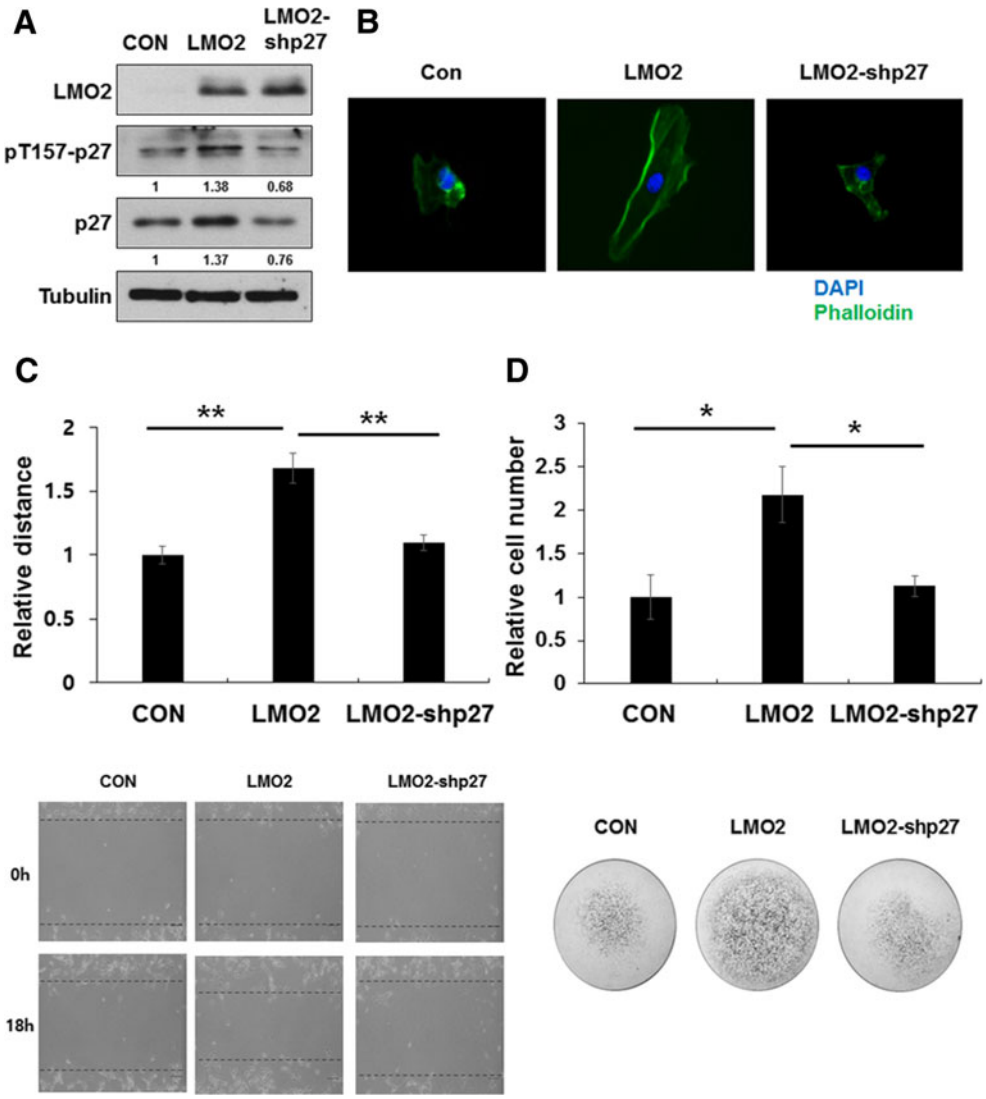

Fig. 4 Knockdown of $p27^{Kip1}$ expression decreases LMO2-driven glioma cell migration and invasion. **a** Levels of total and phosphorylated $p27^{Kip1}$ in U87MG (CON), U87MG-LMO2 (LMO2), and U87MG-LMO2 cells treated with short hairpin RNAs specific for $p27^{Kip1}$ (LMO2-shp27) were examined by western blotting. Protein expression levels were quantified using ImageJ software. **b** Changes in the F-actin network of CON, LMO2, and LMO2-shp27 cells were assessed using immunofluorescence assays employing phalloidin antibody. Images are at ×400 magnification. **c** The in vitro migratory abilities of CON, LMO2, and LMO2-shp27 cells were examined using wound-healing assays. $^{**}P<0.01$ ($n=3$). Representative images of wound healing assay are shown below. **d** The invasiveness of CON, LMO2, and LMO2-shp27 cells was determined in vitro using transwell invasion assays. $^{*}P<0.05$ ($n=3$). Representative images of transwell invasion assay are shown below

healing assays showed that the in vitro migratory ability of U87MG-LMO2 cells was adversely affected by the knockdown of $p27^{Kip1}$ (Fig. 4c). Results from transwell assays showed that the invasiveness of U87MG-LMO2 cells was also significantly decreased when $p27^{Kip1}$ expression was knocked down (Fig. 4d). These findings appear to indicate that LMO2 promotes glioma cell migration and invasion through increases in $p27^{Kip1}$ levels.

Discussion

In a previous study, it was shown that LMO2 expression is elevated in HGG tissues and that this correlated with a poor prognosis for HGG patients [24]. HGG cell invasion and dissemination in surrounding brain tissues are considered the main reasons for the devastating outcomes of glioma after conventional therapy. The recurrence of glioma following the completion of conventional therapies is due to infiltrating glioma cells. Therefore, understanding the mechanisms underlying glioma migration and invasion would assist in preventing glioma recurrence posttherapy. In our current study, we attempted to elucidate the molecular mechanisms underlying LMO2-driven glioma migration and invasion. LMO2 promotes glioma cell migration and invasion by stabilizing cytosolic $p27^{Kip1}$ and by increasing the level of interaction between $p27^{Kip1}$ and RhoA. It is likely that poor clinical outcomes of HGG patients with high LMO2 levels correlated with elevated migration and invasion of glioma cells.

The migration and invasion of cells are orchestrated by several cellular processes, such as cytoskeleton remodeling, protrusion of the leading edge, cell-matrix interaction, extracellular matrix remodeling, cell contraction, and detachment of the trailing edge [31]. Although cell migration and invasion require multi-step events, our results suggest that one of the rate-limiting events for LMO2-mediated cell migration and

invasion involves increased levels of cytosolic $p27^{Kip1}$. Like total and phosphorylated $p27^{Kip1}$, levels in $p27^{Kip1}$-depleted U87MG-LMO2 cells were similar to those in U87MG cells, cell migration, and invasion of $p27^{Kip1}$-depleted U87MG-LMO2 cells that were decreased to levels similar to those seen for U87MG cells (Fig. 4).

The subcellular localization of $p27^{Kip1}$ plays a crucial role in human tumors. Nuclear $p27^{Kip1}$ inhibits the cell cycle by suppressing the activity of cyclin-CDK complexes, whereas cytosolic $p27^{Kip1}$ augments cell migration and invasion by modulating actin filament dynamics, via its interaction with Rho GTPase. One of the key events for cytosolic $p27^{Kip1}$ localization is the phosphorylation of one of three amino acid residues (serine10, threonine157, or threonine198) [32]. In particular, the phosphorylation of $p27^{Kip1}$ at threonine157 by AKT leads to its retention in the cytoplasm [33]. Furthermore, the nuclear localization of threonine157-phosphorylated $p27^{Kip1}$ is reduced via interactions with the 14-3-3 protein [34]. In addition, we observed that there was no change in $p27^{Kip1}$ mRNA levels by LMO2, while phosphorylated AKT and $p27^{Kip1}$ were increased in the LMO2-overexpressing cells. Because AKT phosphorylates and stabilizes $p27^{Kip1}$, it is likely that LMO2 augments cytosolic $p27^{Kip1}$ levels through increased protein stability. In our current study, we did not show the molecular mechanisms that LMO2 directly increases threonine157-phosphorylation of $p27^{Kip1}$ protein. However, our study suggested that LMO2-driven phosphorylation of $p27^{Kip1}$ is a crucial event with respect to glioma migration and invasion and that identification of the responsible mechanism(s) is required to develop an effective plausible therapeutic modality targeting LMO2-driven glioma invasion.

Acknowledgments We are grateful to all members of the Cell Growth Regulation Laboratory for their helpful discussion and technical assistance. This work was supported by grants from Next-Generation Biogreen21 Program (PJ01107701) and the National Research Foundation of Korea (NRF) and the Ministry of Education, Science, and Technology of Korea (2011–0017544).

Conflicts of interest None

References

1. Wen PY, Kesari S. Malignant gliomas in adults. N Engl J Med. 2008;359:492–507.
2. Huse JT, Holland EC. Targeting brain cancer: advances in the molecular pathology of malignant glioma and medulloblastoma. Nat Rev Cancer. 2010;10:319–31.
3. Drappatz J, Norden AD, Wen PY. Therapeutic strategies for inhibiting invasion in glioblastoma. Expert Rev Neurother. 2009;9:519–34.
4. Hoelzinger DB, Demuth T, Berens ME. Autocrine factors that sustain glioma invasion and paracrine biology in the brain microenvironment. J Natl Cancer Inst. 2007;99:1583–93.
5. Chamberlain MC. Radiographic patterns of relapse in glioblastoma. J Neuro-Oncol. 2011;101:319–23.
6. Mattila PK, Lappalainen P. Filopodia: molecular architecture and cellular functions. Nat Rev Mol Cell Biol. 2008;9:446–54.
7. Raftopoulou M, Hall A. Cell migration: Rho GTPases lead the way. Dev Biol. 2004;265:23–32.
8. Abraham MT, Kuriakose MA, Sacks PG, Yee H, Chiriboga L, Bearer EL, et al. Motility-related proteins as markers for head and neck squamous cell cancer. Laryngoscope. 2001;111:1285–9.
9. Kamai T, Tsujii T, Arai K, Takagi K, Asami H, Ito Y, et al. Significant association of Rho/ROCK pathway with invasion and metastasis of bladder cancer. Clin Cancer Res. 2003;9:2632–41.
10. Yan B, Chour HH, Peh BK, Lim C, Salto-Tellez M. RhoA protein expression correlates positively with degree of malignancy in astrocytomas. Neurosci Lett. 2006;407:124–6.
11. Tran NL, McDonough WS, Savitch BA, Fortin SP, Winkles JA, Symons M, et al. Increased fibroblast growth factor-inducible 14 expression levels promote glioma cell invasion via Rac1 and nuclear factor-kappaB and correlate with poor patient outcome. Cancer Res. 2006;66:9535–42.
12. Valge-Archer VE, Osada H, Warren AJ, Forster A, Li J, Baer R, et al. The LIM protein RBTN2 and the basic helix-loop-helix protein TAL1 are present in a complex in erythroid cells. Proc Natl Acad Sci U S A. 1994;91:8617–21.
13. Wadman I, Li J, Bash RO, Forster A, Osada H, Rabbitts TH, et al. Specific in vivo association between the bHLH and LIM proteins implicated in human T cell leukemia. EMBO J. 1994;13:4831–9.
14. Grutz GG, Bucher K, Lavenir I, Larson T, Larson R, Rabbitts TH. The oncogenic T cell LIM-protein Lmo2 forms part of a DNA-binding complex specifically in immature T cells. EMBO J. 1998;17:4594–605.
15. Xu Z, Huang S, Chang LS, Agulnick AD, Brandt SJ. Identification of a TAL1 target gene reveals a positive role for the LIM domain-binding protein Ldb1 in erythroid gene expression and differentiation. Mol Cell Biol. 2003;23:7585–99.
16. Gering M, Yamada Y, Rabbitts TH, Patient RK. Lmo2 and Scl/Tal1 convert non-axial mesoderm into haemangioblasts which differentiate into endothelial cells in the absence of Gata1. Development. 2003;130:6187–99.
17. Mead PE, Deconinck AE, Huber TL, Orkin SH, Zon LI. Primitive erythropoiesis in the Xenopus embryo: the synergistic role of LMO-2 SCL and GATA-binding proteins. Development. 2001;128:2301–8.
18. Pardanaud L, Yassine F, Dieterlen-Lievre F. Relationship between vasculogenesis, angiogenesis and haemopoiesis during avian ontogeny. Development. 1989;105:473–85.
19. Sheaff RJ, Groudine M, Gordon M, Roberts JM, Clurman BE. Cyclin e-cdk2 is a regulator of p27kip1. Genes Dev. 1997;11:1464–78.
20. Boehm M, Yoshimoto T, Crook MF, Nallamshetty S, True A, et al. A growth factor-dependent nuclear kinase phosphorylates p27(kip1) and regulates cell cycle progression. EMBO J. 2002;21:3390–401.
21. Connor MK, Kotchetkov R, Cariou S, Resch A, Lupetti R, et al. Crm1/ran-mediated nuclear export of p27(kip1) involves a nuclear export signal and links p27 export and proteolysis. Mol Biol Cell. 2003;14:201–13.
22. Larrea MD, Liang J, Da Silva T, Hong F, Shao SH, et al. Phosphorylation of p27kip1 regulates assembly and activation of cyclin d1-cdk4. Mol Cell Biol. 2008;28:6462–72.
23. Besson A, Gurian-West M, Schmidt A, Hall A, Roberts JM. p27Kip1 modulates cell migration through the regulation of RhoA activation. Genes Dev. 2004;18:862–76.
24. Kim SH, Kim EJ, Hitomi M, Oh SY, Jin X, Jeon HM, et al. The LIM-only transcription factor LMO2 determines tumorigenic and

angiogenic traits in glioma stem cells. Cell Death Differ. 2015;22: 1517–25.
25. Jin X, Jin X, Sohn YW, Yin J, Kim SH, Joshi K. Blockade of EGFR signaling promotes glioma stem-like cell invasiveness by abolishing ID3-mediated inhibition of p27(KIP1) and MMP3 expression. Cancer Lett. 2013;328:235–42.
26. Dignam JD, Lebovitz RM, Roeder RG. Accurate transcription initiation by RNA polymerase II in a soluble extract from isolated mammalian nuclei. Nucleic Acids Res. 1983;11:1475–89.
27. Kim JK, Jin X, Sohn YW, Jin X, Jeon HY, Kim EJ, et al. Tumoral RANKL activates astrocytes that promote glioma cell invasion through cytokine signaling. Cancer Lett. 2014;353:194–200.
28. Shin I, Yakes FM, Rojo F, Shin NY, Bakin AV, et al. Pkb/akt mediates cell-cycle progression by phosphorylation of p27(kip1) at threonine 157 and modulation of its cellular localization. Nat Med. 2002;8:1145–52.
29. Viglietto G, Motti ML, Bruni P, Melillo RM, D'Alessio A, et al. Cytoplasmic relocalization and inhibition of the cyclin-dependent kinase inhibitor p27(kip1) by pkb/akt-mediated phosphorylation in breast cancer. Nat Med. 2002;8:1136–44.
30. Parker KK, Brock AL, Brangwynne C, Mannix RJ, Wang N, Ostuni E, et al. Directional control of lamellipodia extension by constraining cell shape and orienting cell tractional forces. FASEB J. 2002;16:1195–204.
31. Friedl P, Wolf K. Tumour-cell invasion and migration: diversity and escape mechanisms. Nat Rev Cancer. 2003;3:362–74.
32. Viglietto G, Motti ML, Fusco A. Understanding p27(kip1) deregulation in cancer: down-regulation or mislocalization. Cell Cycle. 2002;1:394–400.
33. Motti ML, De Marco C, Califano D, Fusco A, Viglietto G. Akt-dependent T198 phosphorylation of cyclin-dependent kinase inhibitor p27kip1 in breast cancer. Cell Cycle. 2004;3:1074–80.
34. Sekimoto T, Fukumoto M, Yoneda Y. 14-3-3 suppresses the nuclear localization of threonine 157-phosphorylated p27(Kip1). EMBO J. 2004;23:1934–42.